EPJ manuscript No.
(will be inserted by the editor)

Searches for New Particles

Arnulf Quadt[1]

Physikalisches Institut, Universität Bonn, Nußallee 12, 53115 Bonn

Received: date / Revised version: date

Abstract. Searches for New Particles including future sensitivity prospects are reviewed. The main focus is placed on results obtained at LEP, HERA and the Tevatron on generic searches such as searches for excited fermions, searches for leptoquarks and high-p_T leptons. Also interpretations in the context of anomalous single top production via flavour-changing neutral current, large extra space dimensions, supersymmetry, and various searches for Higgs bosons are discussed.

PACS. 12.60.-i Models beyond the standard model – 13.85.Rm Limits on production of particles

arXiv:hep-ph/0312233v2 19 Jan 2004

1 Introduction

In this review searches for new particles are summarized. The main focus is placed on results from current data as well as future expected sensitivities, where relevant, from LEP, HERA and the Tevatron. This review covers direct searches for particles in and beyond the Standard Model, while indirect constraints on physics beyond the Standard Model from precision electroweak data are mostly described in [1]. Future prospects on searches for new particles at the LHC and/or a linear collider (LC) are summarized in more detail in [2].

Selected topics and recent results are being reviewed. Firstly two examples of generic searches, motivated by the observed structure in the fermion sector are discussed, namely the search for excited fermions and the search for leptoquarks, followed by searches for anomalous single-top production, large extra space dimensions, searches for supersymmetry and various searches for Higgs bosons [1].

2 Excited Fermions

Charged (e^*, μ^*, τ^*) and neutral $(\nu_e^*, \nu_\mu^*, \nu_\tau^*)$ excited leptons are predicted by composite models where leptons and quarks have substructure [3]. These models address fundamental questions left open by the Standard Model, such as the number of three observed fermion families, the hierarchy in the fermion mass values, and the similarity in the electric charge and weak properties of the fermions. A consequence of the possible fermion compositeness or substructure would be the existence of excited fermion states with masses of the exited state in the order of 100 GeV, which are expected to be accessible to various experiments. The most commonly use phenomenological model [3] is based on the assumption that the excited fermions have spin and isospin $\frac{1}{2}$ and both left-handed, F_L^*, and right-handed components, F_R^*, are in a weak isodoublets. The Lagrangian describes the transitions between known fermions, F_L, and excited states:

$$\mathcal{L}_{\mathcal{F}^*\mathcal{F}} = \frac{1}{\Lambda}\overline{F_R^*}\sigma^{\mu\nu}\left[g\, f\, \frac{\boldsymbol{\tau}}{2}\partial_\mu \boldsymbol{W_\nu} + g'\, f'\, \frac{Y}{2}\partial_\mu B_\nu + g_s\, f_s\, \frac{\lambda^a}{2}\partial_\mu G_\nu^a\right] F_L + h.c. \quad (1)$$

where Λ is the compositeness scale; $\boldsymbol{W_\nu}$, B_ν and G_ν^a are the SU(2), U(1) and SU(3) fields; $\boldsymbol{\tau}, Y$ and λ^a are the corresponding gauge-group generators; and g, g' and g_s are the coupling constants. The free parameters f, f' and f_s are weight factors associated with the three gauge groups and depend on the specific dynamics describing the compositeness. For an excited fermion to be observable, Λ must be finite and at least one of f, f' and f_s must be non-zero. By assuming relations between f, f' and f_s, the branching ratios of the excited-fermion decays can be fixed, and the cross section depends only on f/Λ and on the mass of the excited fermion, m_{f^*}.

For the example of excited electrons, the conventional relation $f = f'$ is adopted. Searches for excited electrons have been carried out at HERA in single e^* production with subsequent decays to e, ν and γ, Z, W and at LEP in pair-production, single production, and indirect via t-channel e^*-exchange, i.e. multi-photon events [4]. At low e^*-masses up to the kinematic pair-production limit at LEP close to 100 GeV excited electrons can be ruled out for all values of f/Λ (Figure 1), while in single e^* production searches masses up to $\sqrt{s}$ can be excluded for the coupling f/Λ down to about 10^{-4} GeV^{-1}. Above 300 GeV the best direct exclusion limits have been achieved by the

Send offprint requests to: Arnulf.Quadt@cern.ch

[1] Unless explicitly specified all exclusions limits are quoted at 95% CL.

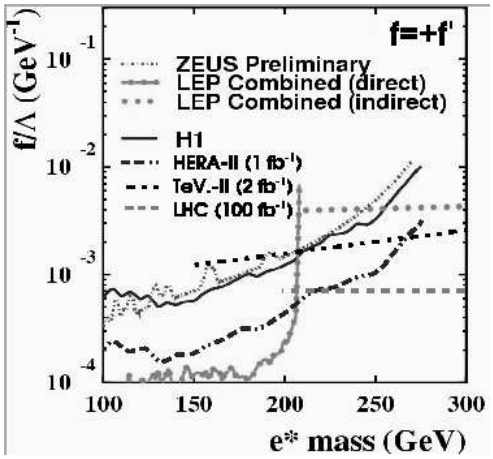

Fig. 1. Upper limits on the coupling f/Λ as a function of the excited lepton mass for HERA and LEP experiments together with the expected sensitivity for HERA-II, Tevatron-II and the LHC.

HERA experiments while at masses beyond 250 GeV the search for t-channel e^* exchange in multi-photon events provides strong indirect limits on f/Λ to be below $\sim 5 \times 10^{-3}$ GeV^{-1}. Preliminary studies show that HERA-II with 1 fb^{-1} will improve the HERA sensitivity by a factor 3-4, the Tevatron with 2 fb^{-1} is expected to have sensitivity down to 2×10^{-3} GeV^{-1} and the LHC with 100 fb^{-1} even down to 7×10^{-4} GeV^{-1} in f/Λ, also at high e^* masses [5]. Similar to their e^* results, the LEP and HERA experiments have also obtained search results for μ^*, τ^* and for ν^*. In the context of contact term production CDF has performed a search for excited electrons with 72 pb^{-1} of Run-II data and excludes masses M_{e^*} up to 785 GeV for $M_{e^*}/\Lambda = 1$.

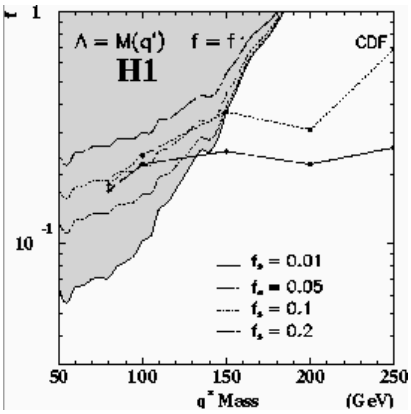

Fig. 2. Upper limits on the coupling f as a function of the excited quark mass for the H1 and CDF experiments for different choices of the relative strong coupling f_s.

The search for excited quark production with de-excitation via radiation of W, Z, γ, gluons is most sensitive at the hadron colliders HERA and Tevatron [6]. For $f = f'$ HERA reaches, depending on the choice of f_s, a sensitivity of down to $f = 0.06$ at low masses of q^*, while studies of the dijet-mass spectra at the Tevatron provide higher sensitivity at large q^* masses (Figure 2). For $f = f' = f_s = 1$ and $\Lambda = M_{q^*}$ DØ in Run-I and CDF in Run-II reach exclusions of up to 775 GeV and 760 GeV, respectively, while a mass exclusion sensitivity for 2 fb^{-1} data of up to 940 GeV is expected. In the coming years further sensitivity improvements are expected from the continuing data taking of the hadron collider experiments. Further details of searches for excited fermions can be found in [7].

3 Leptoquarks

The known symmetry between the lepton and quark sectors could possibly be an indication that they are fundamentally connected through a new interaction. Models for such interactions predict the existence of Leptoquarks (LQs) which are colour-triplet scalar (S) or vector (V) bosons carrying lepton and baryon numbers, and a fractional electromagnetic charge, Q_{em}. Most collider searches are carried out in the context of effective models, in particular in the Buchmüller, Rückl and Wyler (BRW) model [8]. This model describes leptoquark interactions in a most general effective Lagrangian under the assumption that leptoquarks have renormalizable interactions invariant under SM gauge groups, and that they couple only to gauge bosons and to ordinary fermions. Further assumptions are that leptoquarks conserve leptonic number and baryonic number separately (flavour-diagonal). These assumptions result in leptoquark decay branching ratios to electrons and quarks of 0, 50% or 100%.

First-generation leptoquarks can be resonantly produced at HERA by the fusion of an e beam particle with a q from the proton. This process interfers with t-channel electroweak-boson exchange. At the Tevatron leptoquarks can be pair-produced, independent of the leptoquark coupling λ to electrons and quarks, with subsequent decays to charged lepton or neutrino and a quark. At LEP leptoquarks can be virtually exchanged in the t-channel and result in di-jet final states.

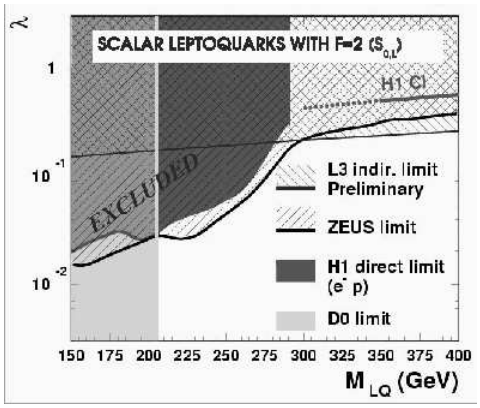

Fig. 3. Constraints from HERA experiments, LEP and DØ in the framework of the BRW model for the example of a leptoquark with fermion number $F = 2$.

Figure 3 shows the results from HERA, LEP and the Tevatron on leptoquark searches [9], in particular choosing here a typical scalar with $F = 2$, namely the $S_{0,L}$ for which $\beta_{eq} = Br(LQ \to eq) = 0.5$. The Tevatron (Run-I) exclusion limit of 204 GeV is independent of λ. For $\lambda \ll 1$, in the mass range beyond the Tevatron reach and below $\sim$ 300 GeV, HERA has the highest sensitivity down to λ of a few $\times 10^{-2}$ which will be superseeded by HERA-II. For leptoquark masses larger than the HERA $\sqrt{s}$ the virtual leptoquark exchange at HERA and LEP provides similar sensitivity to about the electromagnetic strength ($\lambda = \sqrt{4\pi\alpha} \approx 0.3$).

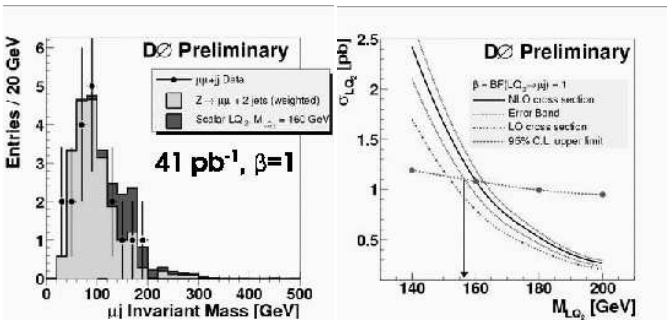

Fig. 4. Left: Invariant μq-mass distribution for early DØ Run-II data in comparison to dominant background and LQ signal. Right: Expected LQ cross section and excluded cross section as a function of LQ mass.

The Tevatron experiments CDF and DØ have already performed searches for scalar leptoquarks in the early Run-II data [9]. In addition to the already established searches for 1st generation leptoquarks, DØ has also searched for 2nd generation leptoquarks. Figure 4 shows the resulting invariant μq mass distribution with a hypothetical signal of 160 GeV along with the expected signal cross section and the experimentally excluded cross section as a function of leptoquark masses. While the typical mass exclusions in the different channels range from 107 GeV to 230 GeV (Table 1), they are expected to increase with 2 fb^{-1} of data to $250 - 325$ GeV in the future. Further details of the leptoquark searches can be found in [9].

Table 1. Preliminary Tevatron Run-II mass exclusions in the different channels for 1st and 2nd generation leptoquarks.

experiment	channel (lumi)	$M_{LQ} >$
CDF	$eeqq$ (72 pb^{-1})	230 GeV
	$\nu\nu qq$ (76 pb^{-1})	107 GeV
DØ	$eeqq$ (41 pb^{-1})	179 GeV
	$\mu\mu qq$ (41 pb^{-1})	157 GeV

4 High p_t-Leptons with Large Missing Transverse Momentum and Limits on Anomalous Top Couplings

At the HERA experiments H1 and ZEUS searches for events containing isolated high-p_t leptons and large missing transverse momentum have been performed [10]. A previously reported excess of events in the electron and muon channel by H1 and in the tau channel by ZEUS (Table 2, Figure 5) has been discussed in the context of potential anomalous flavour-changing neutral current (FCNC) single-top production.

Table 2. Observed and expected number of high-p_t lepton events with large missing transverse momentum for H1 (118.3 pb^{-1}) and for ZEUS (130.1 pb^{-1}).

H1	e obs./exp.	μ obs./exp.	combined
$p_T^X > 25$ GeV	$4/1.49 \pm 0.28$	$6/1.44 \pm 0.26$	$10/2.93 \pm 0.49$
$p_T^X > 40$ GeV	$3/0.54 \pm 0.11$	$3/0.55 \pm 0.12$	$6/1.08 \pm 0.22$
ZEUS			τ obs./exp.
$p_T^X > 25$ GeV	$2/2.90 \pm 0.59$	$5/2.75 \pm 0.21$	$2/0.12 \pm 0.02$
$p_T^X > 40$ GeV	$0/0.94 \pm 0.11$	$0/0.95 \pm 0.14$	$1/0.06 \pm 0.01$

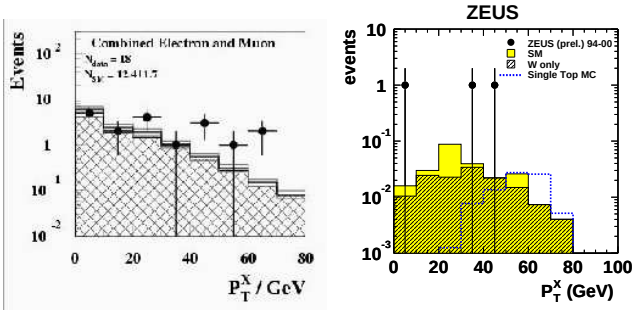

Fig. 5. Distributions of the hadronic transverese momentum p_T^X combined in the electron and muon channel for H1 (left) and in the tau channel for ZEUS (right).

In the SM the neutral currents are flavour diagonal. Flavour-changing neutral currents (FCNC) are not contained at tree level and can happen only from higher-order loop contributions. Sizeable rates can arise only when the top quark appears in the loop. Therefore, no detectable rate is predicted in the SM for FCNC processes between the top and charm or up quarks. However, considerable enhancements are expected, especially at large FCNC [11], in various new models such as models with two or more Higgs doublets, supersymmetric models with or without R-parity conservation, or models with a composite top quark. The top quark phenomenology is less tightly constrained than that of lighter quarks and can be tested at current colliders. In the absence of a specific predictive theory, a most general effective Lagrangian was proposed

to describe FCNC top interactions involving electroweak bosons.

At HERA single-top production can proceed via γ or Z t-channel exchange through anomalous FCNC couplings $\kappa_{tq\gamma}$ or v_{tqZ}, where q is a u- or a c-quark. The sensitivity to couplings for the u-quarks is much higher than that for the c-quark because of the smallness of the c-quark density in the proton, the sensitivity to κ is higher than that to v due to the propagator suppression in the t-channel Z exchange. In comparison to previous analyses the simulation of the Z-exchange process has now been improved allowing an increased sensitivity to FCNC couplings at large v_{tuZ}.

The single-top production at HERA would yield a high-p_T W-boson accompanied by an energetic b-quark jet. When the W decays leptonically the event topology will contain an energetic isolated lepton and large missing transverse momentum, as well as large hadronic transverse momentum, i.e. the topology observed in excess of the SM expectation. For the hadronic decay of the W, the topology will be a three-jet event with a resonant structure in dijet and three-jet invariant masses.

At LEP FCNC single-top quark production has been searched for in the $e^+e^- \to tc(u) \to bWc(u)$ process, where hadronic and leptonic decay modes of the W are considered [11,12]. The LEP experiments have roughly similar sensitivity to κ_γ and v_Z, which increases with lower top quark mass. At the Tevatron, CDF has performed a search for FCNC in the top decays $t \to \gamma c(u)$ and $t \to Zc(u)$ in $p\bar{p}$ collisions [11,13]. The resulting limits on the top quark decay branching ratios have been converted into limits on the FCNC couplings κ_γ and v_Z.

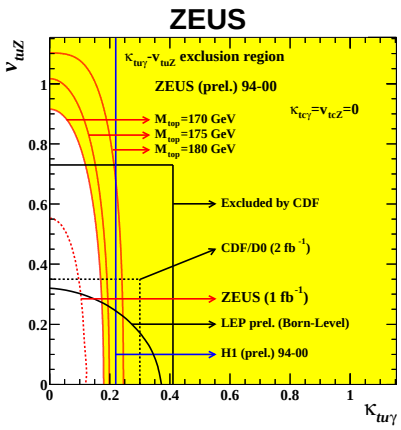

Fig. 6. Exclusion regions in the $\kappa_{tu\gamma} - v_{tuZ}$ plane as achieved by the different experiments along with the expected sensitivity for future data taking at HERA and the Tevatron.

Figure 6 shows the exclusion regions in the $\kappa_{tu\gamma} - v_{tuZ}$ plane as achieved by the different experiments along with the expected sensitivity for future data taking at HERA and the Tevatron[2]. LEP has the highest sensitivity to v_{tuZ} which is expected to become similar for the Tevatron after Run-IIA [14], whereas HERA-I has the highest sensitivity to $\kappa_{tu\gamma}$, which will be improved even further with HERA-II [15]. The observed excess of events in particular by H1 results in slightly weaker exclusion limits in $\kappa_{tu\gamma}$ compared to ZEUS. The tau events by ZEUS are unlikely to be explained by the hypothesis of single top quark production and are not included in this exclusion plot on FCNC couplings.

5 Large Extra Space Dimensions

The Standard Model of particle physics is an extraordinary scientific achievement, with nearly every prediction confirmed to a high degree of precision. Nevertheless, the SM still has unresolved and unappealing characteristics, including the problem of a large hierarchy in the gauge forces, with gravity being a factor of $10^{33} - 10^{38}$ weaker than the other three forces, raising the question why $M_{Pl}/m_{EW} \sim 10^{15}$ is so large. Viable quantum-gravity scenarios have been constructed [17,18] in which the gravitational force is expected to become comparable to the gauge forces close to the EW scale, eventually leading to (model dependent) effects in the TeV range, observable at high energy colliders [19]: virtual graviton exchange and direct graviton emission.

In the string-inspired Arkani-Hamed, Dimopoulos and Dvali (ADD) scenario [17] whith $n \geq 2$ (6 in string theories) "large" compactified extra dimensions, a gravitational "string" scale M_s is introduced in $(4+n)$ which is related to the usual (effective four-dimensional) Planck scale via $M_{Pl}^2 = R^n\, M_s^{2+n}$, where R is a characteristic (large) size of the n compactified extra dimensions. The gravitons are allowed to propagate in these extra dimensions of finite size R which implies that it will appear in our familiar 4-dimensional universe as a "tower" of massive Kaluza-Klein (KK) excitation states. The exchange of KK towers between SM particles leads to an effective contact interactions with a coupling coefficient $\eta_G = \lambda/M_s^4$. The SM fields are localized to the 4-dimensional space-time. For $r \ll R$ the gravitational potential results from Gauss's law in $(n+4)$ dimensions while for $r \gg R$ it takes the conventional form $V \sim 1/r$. Typical compactification radii are:

$n = 1$	$R \sim 10^{13}$ cm	empirically excluded
$n = 2$	$R \sim 100\ \mu$m $-$ 1 mm	under investigation
$n = 3$	$R \sim 3$ nm	

In the Randall-Sundrum [18] (RS) model only one compact extra dimension is introduced. In a similar way to the ADD model, SM particles and forces are constrained to the 4-dimensional SM brane. Only gravity is allowed

[2] Note that the Lagrangian used by LEP and by HERA experiments differ by a multiplicative factor such that $\kappa_{tu\gamma}^{LEP} = \sqrt{2}\,\kappa_{tu\gamma}^{ZEUS}$ and $v_{tuZ}^{LEP} = \sqrt{2}\,v_{tuZ}^{ZEUS}$; also note that LEP and Tevatron are sensitive to u- as well as c-quark couplings with equal strength.

to propagate into the extra dimension. In this model the hierarchy is not generated by the extra volume, but by a specifically chosen geometry ('warped' geometry). As a direct consequence of the geometry, gravity is mainly located in a distance r_0 at a second brane, the Planck brane, and propagates exponentially damped into the extra dimension. Thus, there is only a small overlap between gravity and SM particles and forces, explaining the weakness of gravity with respect to the electroweak interaction, or the observed mass hierarchy.

Experiments in which deviations from Newton's gravitation law are investigated at short distances usually consider the combined potential energy V due to a modulus force and newton gravity to be written as:

$$V = -\int d\boldsymbol{r_1} \int d\boldsymbol{r_2} \quad \frac{G\rho_1(\boldsymbol{r_1})\rho_2(\boldsymbol{r_2})}{r_{12}} \times \quad (2)$$
$$[1 + \alpha \exp(-r_{12}/\lambda)]$$

with G the gravitational constant, r_{12} the distance between two points $\boldsymbol{r_1}$ and $\boldsymbol{r_2}$ in the test masses, and ρ_1, ρ_2 the mass densities of the two bodies. α is the strength of the new Yukawa force relative to gravity, and λ the range. The present limits on the Yukawa strength α as a function of the range λ, as obtained from sophisticated short distance gravity experiments [20], is shown in Figure 7. For $n = 2$ large extra space dimensions new forces with ranges below ~ 200 μm are excluded.

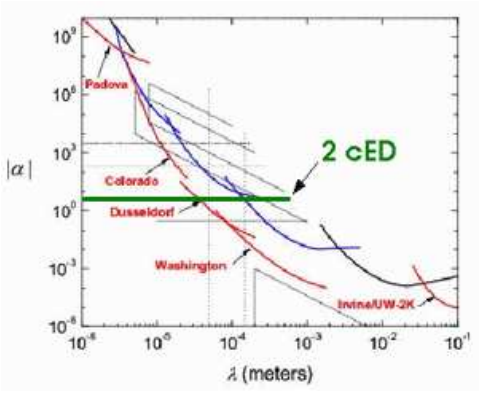

Fig. 7. Current limits on new gravitational strength forces between 1 μm and 10 cm. Shown are the achieved (blue) as well as the in the future expected (red) limits on the Yukawa strength α as a function of the range λ.

5.1 Indirect Effects - Virtual Graviton Exchange

Searches for virtual graviton exchange in theories with large extra dimensions have been performed at HERA, LEP and the Tevatron. At HERA virtual graviton exchange modifies the Q^2 distribution of neutral current events in a characteristic way. Figure 8 shows the ratio of high-Q^2 NC DIS events from H1 to the SM, together with the effect of Kaluza-Klein graviton exchange for the just excluded fundamental scale M_s. The coupling λ, which depends on the full theory and is expected to be of order unity, has been fixed by convention to $\lambda = \pm 1$. Combining both $\lambda = -1$ and $\lambda = +1$ typical limits from H1 and ZEUS are $M_s > 0.8$ TeV.

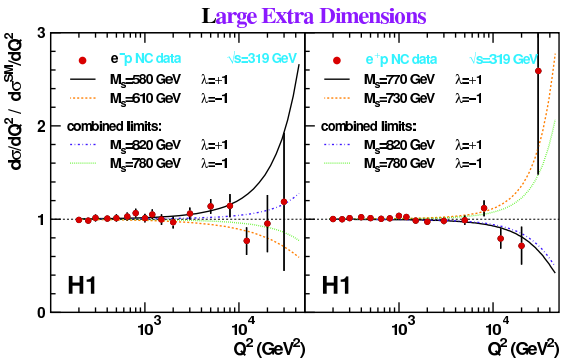

Fig. 8. Constraints for models with large extra dimensions from Q^2 distribution of NC-DIS events at HERA, here H1.

Indirect effects from virtual graviton exchange in large extra dimensions at LEP are searched for in boson (γ, Z) and fermion pair production, taking the modified mass and angular distribution of the final state particles into account. Typical limits obtained for the combination of the LEP data are $M_s > 1.26$ TeV for $\lambda = +1$ and $M_s > 0.96$ TeV for $\lambda = -1$.

At the Tevatron virtual graviton exchange, expected to modify the invariant mass and angular distributions of the final state particles, is searched for in boson (γ, Z) and fermion (e, μ) pair production (Figure 9). Typical limits obtained by CDF or DØ are $M_s > 0.79 - 1.28$ TeV, depending of the channel and data set (Run-I or Run-II).

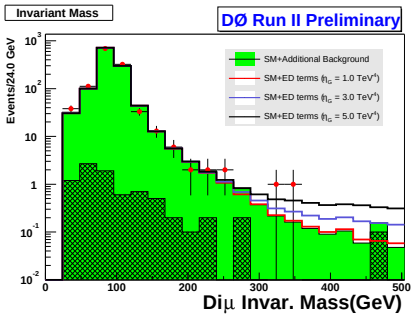

Fig. 9. Comparison of invariant $\mu\mu$ mass distribution between data (30 pb^{-1} DØ data; points) and background (histograms) together with the modifications expected in the presence of large extra space dimensions at high $m_{\mu\mu}$.

5.2 Direct Effects - Real Graviton Emission

Searches for direct effects of large extra dimensions, namely the real graviton emission, have been performed at LEP

and the Tevatron. Real gravitons can be emitted in association with photons or gluons, resulting in large missing transverse momentum and a single photon or gluon, i.e. a monojet.

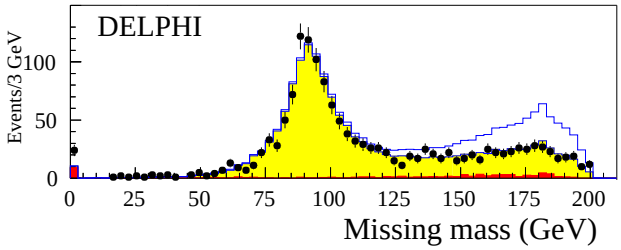

Fig. 10. Missing mass (or recoil mass) distribution of all single photon events in DELPHI. The light shaded area is the expected distribution from $e^+e^- \to \nu\bar{\nu}\gamma$, the dark shaded area is the total background from other sources. The expected signal $e^+e^- \to \gamma G$ production is indicated.

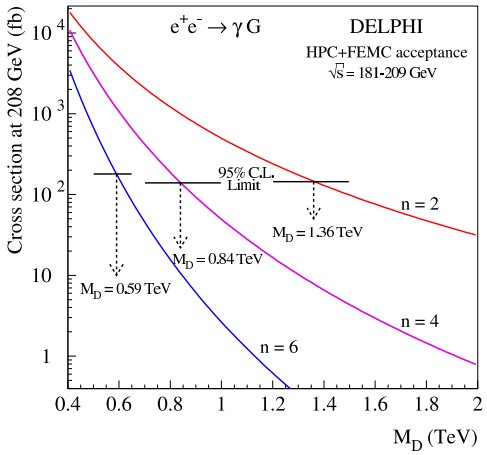

Fig. 11. DELPHI limit and expected cross section for $e^+e^- \to \gamma G$ for 2, 4, and 6 extra dimensions.

Figure 10 shows the missing mass (or recoil mass) distribution of all single photon events in DELPHI (from data recorded at $\sqrt{s} = 181-209$ GeV). The light shaded area is the expected distribution from $e^+e^- \to \nu\bar{\nu}\gamma$ and the dark shaded area is the total background from other sources. The expected signal $e^+e^- \to \gamma G(n = 2, M_D = 0.75$ TeV) production is indicated. This high statistics measurement and the well controlled SM background allow to set cross section limits on the γG production as a function of the fundamental scale M_D. Figure 11 shows the result for the DELPHI experiment for $n = 2, 4$ and 6 large extra dimensions along with the expected cross section. For $n = 2$ extra dimensions $M_D > 1.36$ TeV which corresponds to $R < 260$ μm and for $n = 4$ extra dimensions $M_D > 0.84$ TeV which corresponds to $R < 13$ pm. So the collider experiments reach or already supersede the sensitivity of the short distance gravity experiments.

At the Tevatron direct graviton emission would manifest itself via the production of single jets e.g. from gluons (monojets) along with large missing transverse momentum. CDF and DØ have searched for such topologies in the Run-I as well as in the Run-II data. In the absence of a signal exclusion limits of about $M_S^{n=2} > 1$ TeV have been set. Table 3 summarizes the searches for large extra dimensions at the Tevatron in the various search channels. With the continuing data taking of the Run-II further significant improvements in sensitivity are expected.

Table 3. Summary of searches for large extra dimensions at the Tevatron along with resulting limits on fundamental scale in the ADD or RS model.

experiment		channel	limit
CDF-I	(110 pb^{-1})	di-EM (e,γ)	$M_s > 0.94$ TeV
CDF-I	(87 pb^{-1})	Mono-Jet/γ+$\not\!\!E_T$	$M_s^{n=2} > 1.0$ TeV
CDF-I	(87 pb^{-1})	Mono-Jet/γ+$\not\!\!E_T$	$M_s^{n=6} > 0.6$ TeV
CDF-II	(75 pb^{-1})	Di- e,μ, γ, Jet)	k/M_s limits in RS
DØ-I	(127 pb^{-1})	Di-EM (e,γ)	$M_s > 1.2$ TeV
DØ-I	(78.8 pb^{-1})	Mono-Jet + $\not\!\!E_T$	$M_s^{n=2} > 1.0$ TeV
DØ-I	(78.8 pb^{-1})	Mono-Jet + $\not\!\!E_T$	$M_s^{n=6} > 0.65$ TeV
DØ-II	(120 pb^{-1})	Di-EM (e,γ)	$M_s > 1.28$ TeV
DØ-II	(30 pb^{-1})	Di-μ	$M_s > 0.79$ TeV

5.3 Search for Radions and Branons

In the framework of the Randall-Sundrum model massless and massive spin-two excitations are predicted. The massless excitations couple with gravitational strength and can be identified with gravitons. The masses and couplings of the massive spin-two excitations are set by the weak scale. These states have not yet been observed and should, if existent in nature, become visible with the next generation of colliders. The spinless excitations, called *radions*, correspond to a local fluctuation of the brane distance: $r_0 \to r_0 + \Delta r(x)$. A mechanism has been proposed to stabilize the brane distance, which is required to avoid the branes to drift apart faster than compatible with cosmological models and observations. The radion acquires a mass due to this stabilization mechanism, which is a free parameter. The radion mass is expected to be well below 1 TeV and most likely lighter than massive spin-two excitations. If the Randall-Sundrum model describes nature the radion is expected to be the first sign of it which can be observed.

The radion carries the same quantum numbers as the Higgs boson, so that these two particles can mix. A first search for radions has been performed by OPAL [21], exploiting that the radion as well as the SM Higgs boson are mainly produced in the Higgsstrahlung process $e^+e^- \to Zr$ or $\to Zh$. Limits on the Higgsstrahlung cross section obtained from searches for the SM Higgs boson, flavour-independent searches for hadronically decaying Higgs bosons and decay mode independent searches for Higgs bo-

sons are used to restrict the parameter space of the RS model. As shown in Figure 12 the data excludes masses for the Higgs-like state below 58 GeV for all scales $\Lambda_W \geq$ 246 GeV independent of the mixing between the radion and the Higgs boson, and the radion mass m_r in the range 1 MeV to 1 TeV. The analyses are sensitive to the radion only for scales $\Lambda_W \leq 0.8$ TeV. No universal limits on the mass of the radion-like state can be extracted as they depend on the mixing parameter ξ.

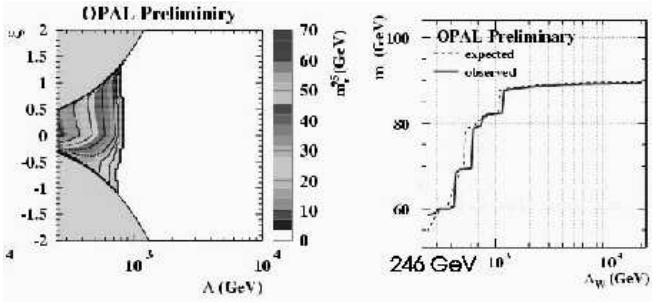

Fig. 12. Left: Observed radion mass limit as a function of the mixing parameter ξ and the fundamental scale Λ_W; Right: Lowest expected and observed limit on the Higgs boson mass as a function of the scale parameter Λ_W for all allowed ξ and for masses of the radion-like state m_r.

In the context of the ADD model new particle fields, called 'branons' are expected and associated with brane fluctuations along the extra dimensions. The dynamics of these fields is determined via an effective theory with couplings of order of the brane tension scale, f. The search for Kaluza Klein gravitons and the search for branons are complementary. If the brane tension is below the gravity scale, $f \ll M_S$, the first signal of extra dimensions will come from branons, allowing a measurement of f, the number of branons and their masses M. If $f \gg M_s$, then the first evidence for extra dimensions will be the discovery of gravitons, giving information about the fundamental scale of gravitation (M_s) and the characteristics of the extra-space (number of dimensions (D), size (R_B), topology etc.).

Branons have a well defined effective theory with couplings to Standard Model particles. Since processes involving the production of only one branon are forbidden by Lorentz invariance the lowest order branon interaction, which has been investigated by the L3 Collaboration [22], is $e^+e^- \to \hat{\pi}\hat{\pi}\gamma$, resulting in a single-photon final state. Comparing the photon energy and angular distributions with the expectation of SM or branon production limits have been placed in the (f, M) plane (see Figure 13) at 95% CL ($R < 0.05$) and at 99% CL ($R < 0.01$). Assuming a flexible brane ($f \ll M$) the single-γ analysis with L3 data imposes the restriction: $f > 206$ GeV, a similar single-Z one: $f > 47$ GeV. Both limits are stronger than the most stringent astrophysical constraint from the energy loss observation in SN1987A; $f > \mathcal{O}(10)$ GeV.

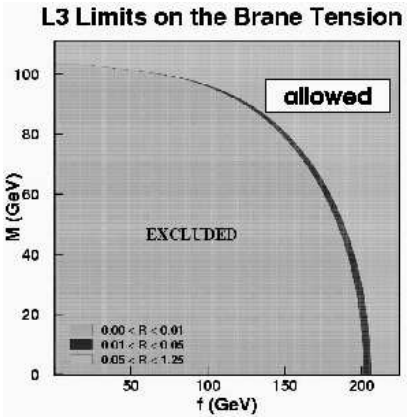

Fig. 13. Two-dimensional limits in the (f, M) plane from the analysis of L3 single photon data. For very elastic branes, $f \to 0$, the exclusion interval for the branon mass is $M \geq 103$ GeV.

Further details on searches for large extra dimensions, radions and branons can be found in [23] and references therein.

6 Searches for Supersymmetry

Supersymmetric (SUSY) extensions of the Standard Model, introducing a symmetry between fermions and bosons, are particularly attractive as they address various shortcomings of the Standard Model such as quadratic divergences in the Higgs mass (cancel in SUSY), the fine tuning problem, the hierarchy problem, coupling unification at very large scales etc. As the supersymmetric partner particles of the known Standard Model particles are not observed, SUSY must be broken. Different models for the SUSY breaking mechanism have been considered, in particular the minimal supersymmetric extension of the Standard Model (MSSM), where the communication between the SUSY breaking sector and our world is either established via gauge bosons (gauge mediated SUSY breaking - GMSB with 6 parameters) or via gravity (gravity mediated SUSY breaking - mSUGRA with 5 parameters). Also R-parity violating SUSY models, where the SUSY particles are not necessarily produced or decay in pairs, are considered. A very large number of topologies has been predicted and searched for in the context of SUSY in the recent years. Here only two examples are discussed: Searches for stop and sbottom production and limits on chargino and neutralino production. For further details, also on other SUSY searches, see [11, 24, 25].

The states $\tilde{q_L}$ and $\tilde{q_R}$ are the partners of the left-handed and the right-handed quarks. They form squark mass eigenstates ($\tilde{q_1}$ and $\tilde{q_2}$), which are orthogonal combinations of them. The mixing angle $\Theta_{\tilde{q}}$ is defined in such a way that $\tilde{q_1} = \tilde{q_L}\cos(\Theta_{\tilde{q}}) + \tilde{q_R}\sin(\Theta_{\tilde{q}})$ is the lighter squark. Since the off-diagonal elements of the mass matrix are proportional to the mass of the corresponding SM partner, $m_q(A_q - \mu\kappa)$, the mixing is expected to be relevant for the fermions of the third family. In that expression μ is the Higgs mass parameter, A_q the trilinear coupling to the

Higgs sector and $\kappa = \tan\beta$ for down-type, $\kappa = 1/\tan\beta$ for up-type quarks. Therefore the sbottom quark could be light, if $\tan\beta$ is large. A light stop could be realized due to large mass splitting resulting from the large top mass. At hadron colliders stops or sbottoms would be produced via the strong interaction, at LEP electroweakly. The coupling of the stop and sbottom to the Z, and therefore the production cross-section, are maximal for $\Theta_{\tilde{q}} = 0$ and minimal for $\Theta_{\tilde{q}} = 56^0$ and 68^0, respectively.

The decay $\tilde{t} \to t\tilde{\chi}^0$ is expected to be dominant, but due to the large top mass and the limits on $\tilde{\chi}^0$ currently experimentally not accessible. The three-body decay $\tilde{t}_1 \to bl\tilde{\nu}$ via chargino would become the dominant decay mode if kinematically allowed. Figure 14 shows the LEP and DØ exclusions limits in the $(m_{stop}, m_{\tilde{\nu}})$ plane. The LEP limits reach up to $m_{stop} \approx 95$ GeV and close to the kinematic limit of $m_{stop} = m_{\tilde{\nu}} + m_b$, while the Tevatron reach of up to 140 GeV in m_{stop} can only be achieved with 20-30 GeV distance to the kinematic limit. The Tevatron experiments are expected to reach up to 200 GeV in sensitivity with the first 2 fb^{-1} of Run-II data. Similarly search limits of up to 160 GeV have been achieved by the Tevatron experiments for the loop suppressed flavour changing two body decay $\tilde{t}_1 \to c\tilde{\chi}^0_1$. Sbottom quarks $\tilde{b}_1$ are expected to decay into $b\tilde{\chi}^0_1$. The resulting exclusion limits in the $(m_{stop}, m_{\tilde{\chi}})$ plane from LEP reaching close to 100 GeV in $m_{sbottom}$, and CDF, reaching beyond 140 GeV, are shown in Figure 14. The expected sensitivity of the Tevatron experiments with the first 2 fb^{-1} reaches up to 220 GeV in $m_{sbottom}$. Further sbottom quark searches from gluino pair production with subsequent decay $\tilde{b}_1 \to b\tilde{\chi}^0_1$ are being performed by CDF-II and described in [25].

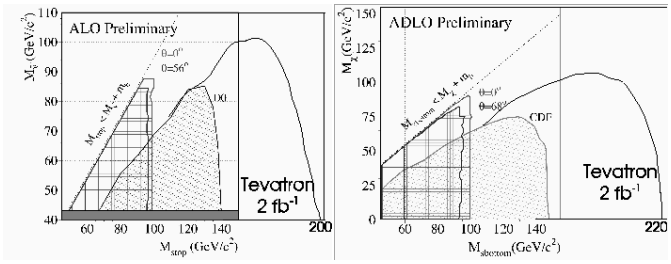

Fig. 14. Left: Stop and sneutrino mass plane showing the regions excluded by LEP, DØ and the expected sensitivity for 2 fb^{-1} at the Tevatron; right: Sbottom and neutralino mass plane showing the regions excluded by LEP, CDF and the expected sensitivity for 2 fb^{-1} at the Tevatron.

Searches for chargino pair production at LEP yielded mass exclusion limits of $m_{\tilde{\chi}^+_1} \geq 103.5$ GeV for $m_{\tilde{\nu}} > 300$ GeV which have been translated into mass limits on the neutralino as a function of $\tan\beta$, assuming SU(5) and SO(10) GUT-relations. In the constrained MSSM, where the neutralino is the lightest SUSY particle (LSP), an absolute mass limit of $m_{LSP} > 46$ GeV is found [26]. If, however, these GUT relations are dropped, assuming for example unification via string theory, no bounds on the neutralino mass can be placed anymore by collider experiments. Assuming, however, the LSP to be the lightest neutralino, to be responsible for the observed cold dark matter relic density and from respecting the LEP2 limits on chargino, slepton and sneutrino masses [27], still a limit of $m_{LSP} > 5$ GeV is obtained. Dropping those assumptions as well, only requiring a possible LSP to be consistent with the observed time dependence of the signal from the supernovae SN1987A, still a limit on the neutralino mass of $m_{LSP} > 100$ MeV can be placed [28].

New collider results are expected soon from the di- and tri-lepton searches at the Tevatron Run-II.

For the first time at a hadron collider, the CDF and DØ Collaborations have observed $Z \to \tau\tau$ signals, where one τ decays leptonically and the other τ is identified in hadronic one- or three-prong decays. This progress in τ-identification, using sophisticated experimental methods, represents a milestone in SUSY and Higgs searches as it opens a sensitivity window to many models and searches for particles coupling to the third fermion generation.

7 Standard Model Higgs Boson Searches

The Higgs mechanism [29] plays a central role in the unification of the electromagnetic and weak interactions by providing mass to the W and Z intermediate vector bosons without violating local gauge invariance. Within the Standard Model, the Higgs mechanism is invoked to break the electroweak symmetry; it requires one doublet of complex scalar fields which leads to the production of a single neutral scalar particle, the Higgs boson. The mass of this particle is not specified, but indirect experimental limits are obtained from precision measurements of the electroweak parameters which depend logarithmically on the Higgs boson mass through radiative corrections. Currently these measurements predict the Standard Model Higgs boson mass to be $m_H = 91^{+58}_{-37}$ GeV and constrain its value to less than 219 GeV at the 95% confidence level [1,30].

7.1 SM Higgs Boson Searches at LEP

The data collected by the four LEP collaborations prior to the year 2000 gave no direct indication of the production of the Standard Model Higgs boson and allowed a lower bound of 107.9 GeV to be set on the mass. During the last year of the LEP programme (the year 2000), substantial data samples were collected at centre-of-mass energies ($\sqrt{s}$) exceeding 206 GeV, extending the search sensitivity to Higgs boson masses of about 115 GeV through the Higgsstrahlung process $e^+e^- \to HZ$. In their initial analyses of the full data sets, ALEPH observed an excess of events consistent with the production of a Standard Model Higgs boson with a mass of 115 GeV; L3 and OPAL, while being consistent with the background hypothesis, slightly favoured the signal plus background hypothesis in this mass region; DELPHI reported a slight deficit with respect to the background expectation.

The final results from the four collaborations have by now been published. These are based on full data reprocessing using final calibrations of the detectors and LEP beam energies, new and improved Monte Carlo generators and increased Monte Carlo event statistics, in some cases, on revised analysis procedures. In total a data set of 2461 pb^{-1} at $\sqrt{s} > 189$ GeV (536 pb^{-1} at $\sqrt{s} > 206$ GeV) has been analysed and combined by the LEP-Higgs working group using the likelihood ratio technique [31].

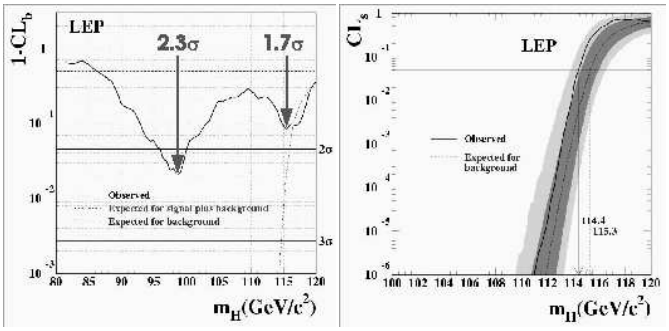

Fig. 15. Left: The background confidence level $1 - CL_b$ as a function of the test mass m_H. The full curve is the observation; the dashed curve is the median expected background confidence and the dashed dotted line is the median expectation for $1 - CL_b$, given the signal plus background hypothesis, when the signal masses on the abscissa is tested. Right: The ratio $CL_s = CL_{s+b}/CL_b$ for the signal plus background hypothesis, as a function of the test mass m_h. The solid line is the observation and the dashed line the median background expectation. The dark and light shaded bands around the median expectation for the background hypothesis correspond to the 68% and 95% probability bands.

In Figure 15 the final results are summarized. Combining the results from the four LEP experiments a lower bound of 114.4 GeV is set on the mass of the Standard Model Higgs boson. The mass limits from the single experiments and the combination are summarized in Table 4. At a mass of 115 GeV, where ALEPH reported an excess compatible with the production of a Standard Model Higgs boson, the confidence $1 - CL_b$ of the combined LEP data expressing the level of consistency with the background hypothesis is 0.9 ($\sim 1.7\sigma$), while the confidence level CL_{s+b} measuring the consistency with the signal plus background hypothesis is 0.15. In the region $m_H \approx 98$ GeV the observed value of $1 - CL_b \approx 0.02$ translates into 2.3 standard deviations. This excess, however, is clearly no sign of Higgs boson production since the number of events expected for such a signal would be a factor of ten larger than the one observed.

The searches for the Standard Model Higgs boson carried out by the four LEP experiments extended the sensitive range well beyond that anticipated at the beginning of the LEP programme. This is due to the higher energy achieved and to more sophisticated detectors and analysis techniques.

Figure 16 shows the development of the direct and the indirect mass bounds over the last years. While the upper mass limit (95% CL) decreased from 1000 GeV to about 200 GeV the best fit value oscillated between 60 and about 150 GeV with a strongly decreasing uncertainty of the electroweak fit. The Higgs boson mass limit from the direct searches at LEP has been steadily increasing from 66 to 114.4 GeV/c^2. The future searches for the Standard Model Higgs boson will concentrate at the low mass region around $110 - 140$ GeV, where the Tevatron experiments have the sensitivity to discover or exclude the Higgs boson before the LHC turns on.

Table 4. Final lower Higgs mass limits of the four LEP-experiments and their combination.

experiment	expected $M_h >$	observed $M_h >$
ALEPH	113.5 GeV	111.5 GeV
DELPHI	113.3 GeV	114.2 GeV
L3	112.4 GeV	112.0 GeV
OPAL	112.7 GeV	112.8 GeV
LEP	115.3 GeV	114.4 GeV

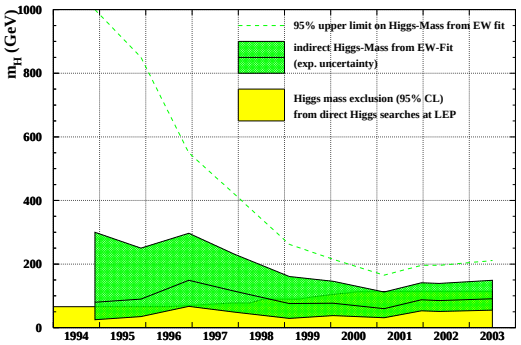

Fig. 16. Development of the upper higgs mass limit (dashed line) and the central value and uncertainty of the electroweak fit (hashed region) over the last years. The light shaded region shows the higgs masses which have been excluded by direct searches for the Higgs boson.

7.2 SM Higgs Boson Searches at the Tevatron

Already the preliminary results on the search for the Standard Model Higgs boson at LEP suggested that the Higgs boson mass may not be very high, which inspired corresponding studies at the Tevatron for Run-II.

The Higgs boson production mechanism with the largest cross section, ~ 0.7 pb for a Higgs mass of 120 GeV, is the gluon fusion. Unfortunately the background in this mode is very large. The most promising Standard Model Higgs discovery channels at the Tevatron are the associated production with W/Z, where the W/Z decay leptonically. The Higgs boson production cross section is $\sim$ 0.16 pb for WH and ~ 0.1 pb for ZH production of a 120 GeV Higgs boson.

Using Run-I data, CDF has searched for WH and ZH in different channels, including Z decaying to dileptons, W decaying to leptons and hadrons and the Higgs decaying to $b\bar{b}$. The results from combining these channels for a

130 GeV Higgs mass gives

$$\sigma(p\bar{p} \to VH) * Br(H \to b\bar{b}) < 7.4 \text{ pb at } 95\%\text{CL} \quad (3)$$

A few years ago, a Tevatron Higgs Working Group's study evaluated the Higgs discovery potential for the Tevatron Run-II [33]. This was a joint effort of theorists and experimentalists from both, the CDF and DØ experiment. The study was based on a parameterized detector simulation. The main conclusions were that in order to maximize the Higgs discovery potential at the Tevatron, one must combine data from both experiments, CDF and DØ; must combine all channels, and must improve the understanding of signal and background processes as well as improve the detector performance. About 2 fb^{-1} of data per experiment were expected to be required for a 95% CL exclusion of a 115 GeV mass Higgs boson, while a 3σ observation was expected to be possible with $5-6$ fb^{-1} and a 5σ discovery with 15 fb^{-1} per experiment. The Tevatron experiments were at the time of this study (1999) expected each to collect 2 fb^{-1} in Run-IIA and 15 fb^{-1} in Run-IIB, i.e. by 2006, so that a discovery would have been possible for a ~ 115 GeV mass Higgs boson and in the absence of a Higgs boson an exclusion potential of up to ~ 180 GeV was estimated.

In the meantime CDF and DØ reviewed and repeated the Higgs sensitivity study [32], taking the projections of the already achieved Run-II performance of the largely and successfully upgraded detectors and the improved understanding of the dominant background sources from data measurements into account. Particular emphasize was given to the calorimeter resolutions on jet-E_T and di-jet mass resolutions as well as the tracking impact parameter resolution, one of the crucial detector parameters for the b-tagging algorithms. The expectations of the initial study [33] are all essentially met, while the analyses techniques and background estimates could be significantly improved. The studies were split up such that CDF reviewed the $WH \to l\nu b\bar{b}$ channel while DØ reviewed the $ZH \to \nu\nu b\bar{b}$ channel. Assuming comparable performance by CDF and DØ the results were then combined. In the following, the $ZH \to \nu\nu b\bar{b}$ analysis is review in more for detail as an example.

This new Higgs sensitivity study was done in two stages: In the first stage the analyses assumptions were left unchanged with respect to the previous study in [33] while the analysis was improved in a number of aspects. In particular:

- The QCD background level was conservatively estimated to be equal to the level of the remaining background sources, i.e. 50% of the total background was assumed to originate from QCD processes.
- The trigger efficiency was assumed to be 100%.
- The b-tagging efficiency was assumed to be 35% for events with one tight and one loose tag, and 32% for events with two tight tags.
- In contrast to [33], where the detector performance was estimated using fast parametrisations, here it was simulated using the full GEANT detector description.
- The analysis was based on a real artificial neural network, while previously it was cut-based.
- The Monte Carlo event samples in the new study were obtained by mixing the hard collision events with five additional minimum bias events overlayed while previously only hard scattering events were considered.

The number of events selected per fb^{-1} in the $ZH \to \nu\nu bb$ analysis for a Higgs of mass 115 GeV is summarized in Table 5. It can clearly be seen that the main change comes from the large reduction in the Zbb and Wbb events, exploiting the separation power of the neural network, resulting in a significant reduction of the total expected background. This translates into a significance increase, estimated in $S/\sqrt{B}$, from 0.78 to 1.12, where the Higgs signal mostly originates from the HZ production but also HW significantly contributes to the $HZ \to bb\nu\nu$ analysis. In other words the integrated luminosity, required for a particular significance, has been reduced by $\sim 50\%$.

In a second stage new cross section estimates, either from improved theory calculations or from measurements using Tevatron data (here upper limits on the cross sections for the Wbb and Zbb process) and an improved description of the analyses was applied. In particular:

- Estimates of realistic trigger efficiencies were applied.
- The QCD background contribution was estimated from data.
- The b-tagging efficiency was assumed to be 35% for events with one tight and one loose tag, and 32% for events with two tight tags.

From the summary in Table 5 it can be seen that the largest improvement comes from the reduction in QCD background, which is to a large extent instrumental background and best estimated from the data itself. This more realistic study results in a significance increase from 0.78 to 0.92, which translates into the integrated luminosity, required for a particular significance, still being reduced by $\sim 28\%$. Given those numbers it should be noticed that:

- At present the double b-tagging efficiency for Run-IIA data has been found to be 19% compared to the 32% expected from the upgrade to the Run-IIB silicon vertex detectors, which is assumed for this as well as the previous study. If the vertex detectors were not upgraded, more luminosity would be needed[3]
- More sophisticated statistical combination techniques as used in the LEP-Higgs search (CL_s method), using mass distributions rather than simple event counting as used here, are expected to reduce the required luminosity for a given sensitivity by $\sim 20\%$.
- More sophisticated analysis techniques are being developed, which are expected to reduce the required data statistics for a given sensitivity even further. See the latest Run-I top mass reanalysis for example [34].

[3] In September 2003 it was decided by the Fermilab Directorate to cancel the Run-IIB silicon vertex upgrade programmes. Consequently the required luminosity for a given Higgs sensitivity is larger and needs to be re-evaluated.

Table 5. Expected number of events per fb^{-1} data in the $ZH \to \nu\nu b\bar{b}$ analysis as estimated at the SUSY/Higgs Workshop in 1999 (SHW 1999), as estimated using the new neural network analysis, but identical cross sections (ANN'03) and as estimated using that new analysis with the latest cross section calculations or estimates from data (Analysis'03).

Process	SHW 1999	ANN'03	Ratio	Analysis'03	Ratio	Comment
HZ(115 GeV)	3.15	3.82	1.22	2.86	0.91	
HW(115 GeV)	2.39	2.78	1.16	2.08	0.87	
$Zb\bar{b}$	4.34	1.73	0.4	1.99	0.46	estimated from CDF data
$Wb\bar{b}$	9.45	3.59	0.38	4.34	0.46	estimated from CDF data
ZZ	1.82	2.36	1.3	2.93	1.61	PYTHIA 6.125 + K-factor=1.34
WZ	1.45	1.79	1.45	1.84	1.27	PYTHIA 6.125 + K-factor=1.34
$t\bar{t}$	3	6.53	2.18	5.48	1.83	average of NLO calculations
qtb	0.31	0.8	2.62	0.68	2.22	NLO calculation
tb	4.7	0.49	0.1	0.35	0.08	NLO calculation
QCD	25.06	17.3	0.69	11.16	0.45	from this study
total background	50.11	34.59		28.77		
significance ($S/\sqrt{B}$)	0.78	1.12		0.92		

– This analysis is still not optimized. Reviewing the $H \to WW$ channels is expected to improve the sensitivity in a similar manner for Higgs boson masses at or above 130 GeV.

Figure 17 shows the result of the new Higgs sensitivity study, combining the CDF and DØ results on the $WH \to l\nu b\bar{b}$ and $ZH \to \nu\nu b\bar{b}$ channels, respectively, and assuming equivalent improvements in the $ZH \to llbb$ channel. At this stage the combination was done using the CL_s method. The largely ($\sim 28\%$) reduced integrated luminosity required for the 95% CL exclusion, the 3σ observation, or the 5σ discovery for a given Higgs boson mass is shown as a function of the Higgs boson mass. Since the analyses concentrated on the decay $H \to b\bar{b}$, improvements with respect to [33] are seen in the Higgs boson mass range up to ~ 130 GeV. Similar potential for improvement at higher masses is expected from a review of the $H \to WW$ decay mode channels. Since this study did not include extensive systematic studies the wide error band, known from the previous study, is not shown.

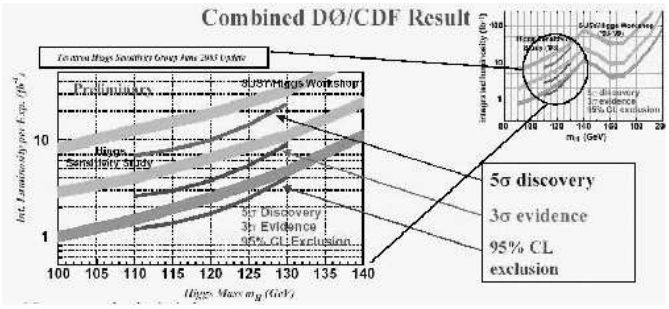

Fig. 17. Integrated luminosity required per experiment, to either exclude a SM Higgs boson at 95% CL or to discover it at the $3\,\sigma$ or the $5\,\sigma$ level at the Tevatron.

Along with this reviewed Higgs sensitivity study by the CDF and DØ collaborations, also the Tevatron luminosity performance and projections have been reviewed.

Table 6. Latest projections on integrated luminosity in fb^{-1} for the Tevatron Run-II in the conservative baseline and in the design scenario.

year	baseline	design
2003	0.28	0.3
2004	0.59	0.68
2005	0.98	1.36
2006	1.48	2.24
2007	2.11	3.78
2008	3.25	6.15
2009	4.41	8.57

Based on the observed Tevatron collider performance compared to the initial luminosity plans, new projections for the integrated luminosity in Run-II have been worked out in a conservative 'baseline' and in the 'design' scenario. These numbers include a shutdown in 2005/2006 for installation of new machine components and optimization and are summarized in Table 6. Depending on the future development of the Tevatron the collider experiments are expected to receive a delivered integrated luminosity between 4.4 fb^{-1} and 8.6 fb^{-1}. These projections in luminosity compensate the improved analysis sensitivity so that overall the Higgs mass region to which the Tevatron experiments are sensitive for exclusion, observation or discovery is somewhat reduced compared to the initial estimate [33].

With the presently available data set the Tevatron experiments have no sensitivity to the Standard Model Higgs boson. Nevertheless, searches for the Higgs boson in the HZ and HW channels are being performed and studied, in particular in the $H \to WW$ channel. A detailed description of the present status is given in [35].

7.3 Higgs Boson Searches at the LHC

The search for the Standard Model Higgs boson is one of the primary tasks of the experiments at the *Large Hadron*

Collider (LHC). It has been established in many studies [36] that a Standard Model Higgs boson can be discovered with high significance over the full mass range of interest, from the lower limit of 114.4 GeV set by the LEP experiments [31] up to about 1 TeV.

At the LHC, the production cross-section for a Standard Model Higgs boson is dominated by gluon-gluon fusion. The second largest cross-section comes from the fusion of vector bosons radiated from initial-state quarks. The relative contributions of the two processes depend on the Higgs boson mass. For $m_H < 2m_Z$, vector boson fusion amounts to about 20% of the total production cross-section and becomes more important with increasing mass. However, for this production mode, additional event characteristics can be exploited to suppress the large backgrounds. The Higgs boson is accompanied by two jets in the forward regions of the detector, originating from the initial quarks that emit the vector bosons. In addition, central jet activity is suppressed due to a lack of colour exchange between the quarks. This is in contrast to most background processes, where there is colour flow in the t-channel. Therefore jet tagging in the forward region of the detector together with a veto of jet activity in the central region are useful tools to enhance the signal-to-background ratio.

The observation of the Standard Model Higgs boson at the LHC in the vector boson fusion channels in the intermediate mass range was first discussed in [37] for the $H \to \gamma\gamma$ and $H \to WW^{(*)}$ decay modes and in [38] for the $H \to \tau\tau$ decay mode. In the recent past ATLAS [39] and CMS [40] have performed analyses for the $WW^{(*)}$ and $\tau\tau$ decay modes using realistic detector simulations of the expected performance of the detectors at the LHC, including forward jet tagging. The performance is addressed at low luminosity, i.e. $\mathcal{L}= 10^{33}$ cm^{-2}s^{-1}. The discovery potential is evaluted for an integrated luminosity up to 30 fb^{-1}, which is expected to be reached during the first few years of operation.

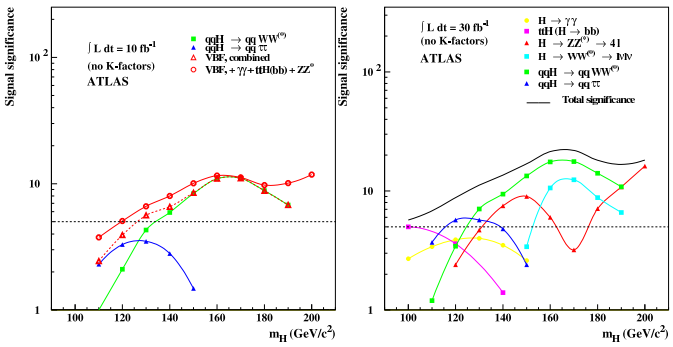

Fig. 18. ATLAS sensitivity for the discovery of a Standard Model Higgs boson for integrated luminosities of 10 and 30 fb^{-1}. The signal significances are plotted for individual channels, as well as for the combination of channels.

In the example of the ATLAS experiment, the resulting sensitivity for a discovery of the Standard Model Higgs boson in the mass range $110-190$ GeV including the vector boson fusion channels is shown in Figure 18 for integrated luminosities of 10 and 30 fb^{-1}. The vector boson fusion channels provide a large discovery potential even for small integrated luminosities. Combining the two vector boson fusion channels, a Standard Model Higgs boson can be discovered with a significance above 5σ in the mass range 135 to 190 GeV assuming an integrated luminosity of 10 fb^{-1} and a systematic uncertainty of $\pm 10\%$ on the background. If the vector boson fusion channels are combined with the standard Higgs boson discovery channels $H \to \gamma\gamma$, $H \to ZZ^{(*)} \to 4l$, and $t\bar{t}H$ with $H \to b\bar{b}$, the 5σ discovery range can be extended down to ~ 120 GeV.

For an integrated luminosity of 30 fb^{-1}, the full mass range can be covered by ATLAS with a significance exceeding 5σ. Over the full mass range several channels, complementary both in physics and detector aspects, will be available for a Higgs boson discovery. The three different channels test different production mechanisms, the gluon-gluon fusion via the $\gamma\gamma$ channel, the vector boson fusion via the WW and $\tau\tau$ channels, and the associated $t\bar{t}H$ production in the $H \to b\bar{b}$ mode. This complementarity also provides sensitivity to non-standard Higgs models, such as fermiophobic models, and allows a measurement of the Higgs boson couplings to fermions [41]. Similar results have been obtained by the CMS Collaboration [40].

In the recent years also on the theoretical understanding of signal and background calculations for the Higgs boson searches at the LHC a lot of progress has been made, in particular on NLO calculations of $pp/p\bar{p} \to t\bar{t}H$ [42], NNLO calculations on the inclusive Higgs production via gg-fusion [43], NLO calculations on background processes for $gg \to \gamma\gamma$ [44], NLO calculations on $bg \to bH$ [45] and WH- and ZH-production [46].

8 Neutral Higgs Boson searches in the MSSM

Numerous theoretical attempts to extend the SM usually lead to the introduction of at least one additional doublet of scalar fields in the Higgs sector. In the minimal supersymmetric extension of the Standard Model (MSSM) this results in 5 Higgs boson mass eigenstates - 3 neutral ($h/H/A$) and 2 charged (H^+ and H^-). In the CP-conserving MSSM, the three neutral Higgs bosons are CP eigenstates: the h and H are CP-even and the A boson is CP-odd since all CP-violating phases in the Higgs sector have been set to zero. Only the CP-even states couple to the Z boson at tree level. Therefore the main Higgs production mechanisms at LEP are the Higgsstrahlung $e^+e^- \to hZ$ and HZ, and the associated production $e^+e^- \to hA$ and HA. Instead of one parameter - the mass of the Higgs boson - the phenomenology is now described by two parameters with the most popular choice of $\tan\beta$ and the mass of the pseudoscalar neutral bosons M_A. At tree level the mass of the lighter CP-even Higgs boson is restricted to be less than the mass of the Z^0. Radiative corrections, in particular from loops containing the top quark, allow the lightest Higgs boson mass to range up to approximately 135 GeV. The combined data of the four LEP experiments are interpreted in the framework of

the 'constrained' MSSM, where in the past three typical benchmark MSSM scans were considered, yielding typical observed (expected) mass limits of $m_h > 91\,(95)$ GeV and $m_A > 92\,(95)$ GeV with $\tan\beta$ exclusions between 0.5-2.4 or 0.7 - 10.5, depending on the benchmark scan. Details on these searches can be found in [47].

In the last years more MSSM benchmark scans have been proposed [48], inspired by Higgs Boson searches at the LHC. Due to the different initial states, the Higgs production and decay channels relevant for Higgs boson searches were different at LEP2 to what they are at hadron colliders. New benchmark scenarios for the MSSM Higgs boson search at hadron colliders have been suggested that exemplify the phenomenology of different parts of the MSSM parameter space. Besides the m_h^{max} scenario and the no-mixing scenario used in the LEP2 Higgs boson searches, two new scenarios have been proposed. In one the main production channel at the LHC, $gg \to h$, is suppressed. In the other, important Higgs decay channels at the Tevatron and at the LHC, $h \to b\bar{b}$ and $h \to \tau^+\tau^-$, are suppressed. First preliminary studies in OPAL [49,50] show that the $h \to b\bar{b}$ suppressed region is kinematically out of reach at LEP2 while a significant part of the parameter space can be excluded. A combination of the LEP data will address these new MSSM benchmark scans in the near future, defining the reference point for future MSSM Higgs boson searches at the LHC.

8.1 CP-Violating MSSM Scenarios

In the MSSM the Higgs potential is assumed to be invariant under CP transformation at tree level. However, it is possible to break CP symmetry in the Higgs sector by radiative corrections, especially by contributions from third generation scalar quarks [51]. Such a scenario is theoretically attractive as it provides a possible solution to the cosmic baryon asymmetry [52], while the CP-violating effects predicted by the SM are too small to account for it.

For the first time the LEP Higgs searches have also been interpreted in the CP-violating MSSM scenario [49]. In such a scenario the three neutral Higgs bosons, $H_i (i = 1,2,3)$ are mixtures of the CP-even and CP-odd Higgs fields. Consequently, they all couple to the Z boson and to each other, and these couplings may be widely different from those of the CP-conserving scenario. In the CP-violating scenario the Higgsstrahlung processes $e^+e^- \to H_iH_j$ $(i \neq j)$ may all occur, with widely varying cross sections. In large domains of the model parameters, the lightest Higgs boson H_1 may escape detection, although it has a predicted mass that is well within the LEP range, since its coupling to the Z boson is too weak for detection; on the other hand, the other two Higgs boson masses can be out of reach or also may have small cross sections. As a result the limits on MSSM parameters advertised so far for the CP-conserving scenario can be invalidated. The decay properties of the Higgs bosons, while being quantitatively different in the two scenarios, maintain a certain similarity. Since Higgs bosons, in general, couple to mass, the largest branching ratios are those to $b\bar{b}$ and $\tau\tau$ pairs. If kinematically allowed, the decays $h \to AA$ (CP-conserving scenario) or $H_2 \to H_1H_1$ (CP-violating scenario) would occur and could even be dominant decays.

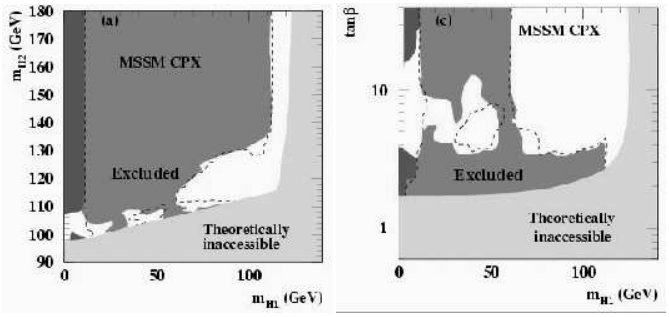

Fig. 19. Preliminary OPAL results on exclusion areas in the CP-violating MSSM. The observed exclusion region is medium shaded (green), the expected excluded region is indicated by the dashed line and the theoretically inaccessible region is light shaded (yellow). Regions excluded by Z width constraints or by decay mode independent searches are dark shaded (red).

Figure 19 shows the preliminary exclusion results of the Higgs search and interpretation in the CP-violating MSSM. In the area of heavy m_{H_2} the lighter H_1 resembles the SM Higgs boson with very little effect from CP-violation (limit on $m_{H_1} > 112$ GeV). In the region below $m_{H_2} \approx 130$ GeV CP violating effects play a major role. Exclusion is obtained for $\tan\beta < 3.2$ and $m_{H_1} < 112$ GeV in the SM like regime. For $4 < \tan\beta < 10$ ZH_2 production is dominant. The large difference between the expected and observed exclusion regions in the area of $4 < \tan\beta < 10$ is mainly due to a less than $2\,\sigma$ excess of events. For light $m_{H_1} < 50$ GeV there are regions expected to be unexcluded, due to the dominant $ZH_2 \to ZH_1H_1$ production with relatively large m_{H_1}, yielding broadened resolutions and therefore reduced sensitivity.

CP-violating MSSM models will also be subject of the upcoming final combination of LEP data by the LEP-Higgs working group.

9 Search for Charged Higgs Bosons

Extensions to the minimal Standard Model contain more than one Higgs doublet. In particular, models with two complex Higgs doublets (2HDM) predict two charged Higgs bosons $H^\pm$. In 2HDM type-II the ratio of the charged Higgs couplings to down- and up-type fermions is given by the ratio of the vacuum expectation values for the two doublets. At born level the charged Higgs mass has to be larger than the W-boson mass. But radiative corrections can reduce the charged Higgs mass below this threshold.

At LEP the search for the charged Higgs boson in $e^+e^- \to H^+H^-$ is performed in the three decay channels $H^+H^- \to \tau^+\nu_\tau\tau^-\bar{\nu}_\tau$, $H^+H^- \to c\bar{s}\tau^-\bar{\nu}_\tau$ and $H^+H^- \to c\bar{s}\bar{c}s$, assumed to be the only possible decays.

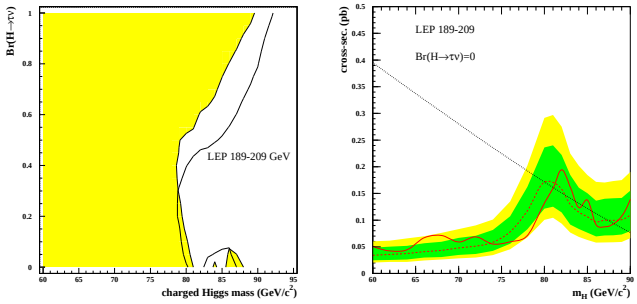

Fig. 20. Left: Preliminary LEP-combined exclusion region in the plane of $Br(H^{\pm} \to \tau\nu)$ and $m_{H^{\pm}}$, using ≈ 2.5 fb^{-1}. Right: Expected cross section for $e^+e^- \to H^+H^-$ production (dotted line), observed cross section limit (full line) and expected cross section limit along with 1 and $2\,\sigma$ error band as a function of the charged Higgs mass.

Figure 20 shows the preliminary LEP-combined results [53] on the exclusion region in the plane of $Br(H^{\pm} \to \tau\nu)$ and $m_{H^{\pm}}$ and , using ≈ 2.5 fb^{-1}. Also shown is the expected signal cross section along with the expected and observed cross section limit as a function of the charged Higgs mass for $Br(H^{\pm} \to \tau\nu) = 0$. The large W-background at about 81 GeV, which also defines the lower mass bound can clearly be seen. At $m_{H^+} \approx 67$ GeV a $\sim 2\,\sigma$ excess is observed, which comes mainly from the L3 data. Within L3 this excess of events has been observed for data from all centre-of-mass energies in all years, summing up to a $\sim 4.6\,\sigma$ excess in the year 2000 [53].

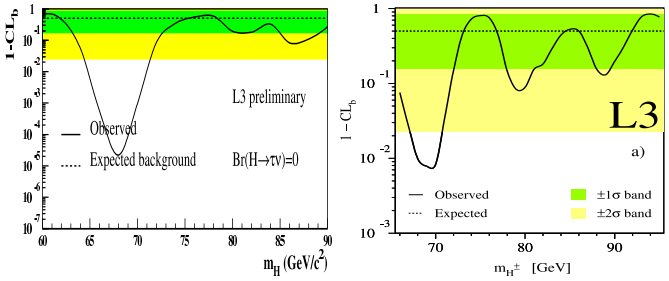

Fig. 21. Left: Confidence level $1-CL_b$ for background-only hypothesis for charged Higgs L3 data from [53] (year 2000). The observed values are shown as solid line, the expected value of 0.5 as dashed line and the 1- and $2-\sigma$ band as shaded regions. An excess of about $4.6\,\sigma$ is observed at $m_{H^{\pm}} \approx 67$ GeV. Right: Confidence level $1 - CL_b$ for background-only hypothesis for latest charged Higgs L3 data from [54]. The excess has been reduced to about $2.4\,\sigma$.

Figure 21 shows the confidence level $1 - CL_b$ for the background-only hypothesis as a function of the charged Higgs mass for the L3 data. The large excess of events, resulting in a strong dip of the confidence level at $m_{H^{\pm}} \approx 67$ GeV can be clearly seen.

In the meantime L3 has reanalysed their data using the latest detector calibration and using the hadronic W-mass for cross checks [54]. In doing so the excess in the new preliminary results has been largely reduced to about 2.4 σ (see Figure 21), resolving the long-standing puzzle on this low-mass excess. The final combination will be performed by the LEP-Higgs working group in the near future.

OPAL has also interpreted a measurement of the ratio of τ-decay branching ratios to muons and electrons in the context of 2HDM type-II and extracted mass limits [55]. The ratio of branching ratios $Br(\tau^- \to \mu^-\bar{\nu}_\mu\nu_\tau)/Br(\tau^- \to e^-\bar{\nu}_e\nu_\tau) = 0.9726\,(1 + 4\eta m_\mu/m_\tau)$ allows a measurement of the Michel parameter η. A non-zero value of η may imply the presence of scalar couplings. In the 2HDM type-II the relation $\eta = -\frac{m_\tau m_\mu}{2}\,(\tan\beta/m_{H\pm})^2$ results in sensitivity of this measurement to $\tan\beta$ and the charged Higgs mass. The OPAL measurement yields a limit of $M_{H^{\pm}} > 1.28\,\tan\beta\,\mathrm{GeV}$, complementing an earlier limit of $M_{H^{\pm}} > 1.89\,\tan\beta\,\mathrm{GeV}$, obtained from studies of $b \to \tau^-\bar{\nu}_\tau X$ decays.

DELPHI has also performed a search for charged Higgs bosons in the context of 2HDM type-I [56], where at $\tan\beta > 1$ the decay $H^{\pm} \to W^*A$ becomes allowed or even dominant, depending on the choice of the CP-odd Higgs mass m_A. The decays of the W to leptons and hadrons are considered while the A predominantly decays to $b\bar{b}$ in the parameter region considered. These new decay channels are combined together with the charged Higgs decays to $c\bar{s}$ and $\tau\nu$ and yield a mass limit of $m_{H^{\pm}} > 76.6$ GeV, independently of $\tan\beta$ for $m_A > 12$ GeV (Figure 22).

Further details and discussion on the status of searches for charged Higgs bosons can be found in [57].

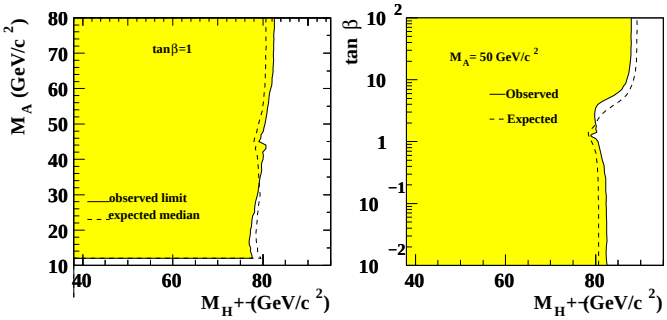

Fig. 22. Typical observed and expected exclusion regions from preliminary DELPHI results in the 2HDM type-I.

10 Fermiophobic Higgs Searches

In 2HDM's without explicit CP-violation the couplings of the Higgs doublets to fermions could be realized in different ways, one possibility is that only one of the doublets couples to fermions. The coupling of the lightest CP-even boson to a fermion pair is then proportional to $\cos\alpha$. If $\alpha = \pi/2$ this coupling vanishes and h^0 becomes a fermiophobic Higgs: it will decay to pairs of other Higgs bosons or massive gauge bosons when kinematically allowed, or to two photons in a large region of the parameter space.

The LEP collaborations have searched for fermiophobic Higgs bosons in the $h \to \gamma\gamma$ and $h \to WW$ channels in the Higgsstrahlung production $e^+e^- \to ZH$ [58]. Lower mass bounds of $m_h > 109.7$ GeV (observed) and $m_h > 109.4$ GeV (expected) have been obtained. Corresponding searches at the Tevatron using Run-I or Run-II data presently have a sensitivity of up to ~ 80 GeV [59].

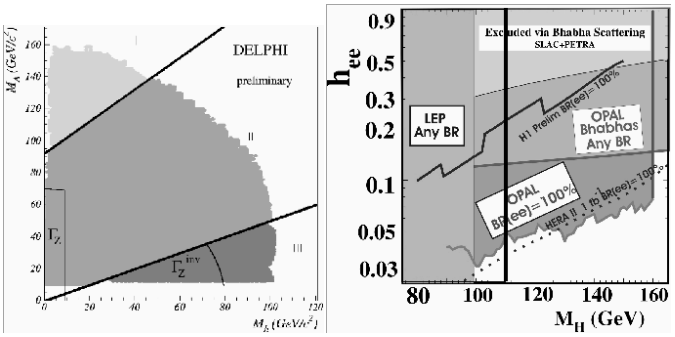

Fig. 23. Left: The shaded areas correspond to the regions excluded for all values of δ. The plot is devided in regions according to the dominant decay modes of h and A; right: Constraints on doubly-charged Higgses in the plane of Yukawa coupling and doubly-charged Higgs mass.

DELPHI has also searched for $e^+e^- \to hA$ with subsequent decays to $h \to \gamma\gamma$ and $A \to b\bar{b}$ or $A \to hZ$ [60]. Also results for $h \to AA$ and for long-lived A are considered. In general 2HDM, the main mechanisms for the production of neutral Higgs bosons at LEP are $e^+e^- \to hZ$ and $e^+e^- \to hA$, both proceeding via Z exchange. The two processes have complementary cross sections proportional to $\sin^2\delta$ and $\cos^2\delta$, respectively, where $\delta = \beta - \alpha$.

The combination of the results on hZ and hA production is shown in Figure 23. The upper limits on $\sin^2\delta$ for a given M_h and the upper limits on $\cos^2\delta$ for a given (M_h, M_A) pair are combined to exclude the (M_h, M_A) pair for all δ values. h masses up to ≈ 100 GeV can be excluded while the sensitivity in M_A reaches up to ≈ 160 GeV.

Further discussionss on fermiophobic Higgs searches can be found in [61].

11 Search for Doubly Charged Higgs Bosons

Some theories beyond the Standard Model predict the existence of doubly-charged Higgs bosons, $H^{\pm\pm}$ with $m_{H^{\pm\pm}} \sim 100$ GeV, including in particular Left-Right symmetric models and Higgs triplet models. It has been particularly emphasized that heavy right-handed neutrinos together with the see-saw mechanism to obtain light neutrinos can lead to a doubly-charged Higgs boson with a mass accessible to current and future colliders. Doubly-charged Higgs bosons would decay into like-signed lepton or vector boson pairs, or with a negligible branching fraction to a W-boson and a singly-charged Higgs boson. For masses less than twice the W-boson mass, they would decay predominantly into like-signed leptons.

Limits on the Yukawa couplings exist from muonium conversion experiments $(\mu^+e^- \to \mu^-e^+)$ $\sqrt{h_{ee}h_{\mu\mu}} \leq 7.6 \cdot 10^{-3}\ \mathrm{GeV}^{-1}\,\mathrm{M_H}$ and from avoiding large contributions to $(g-2)_\mu$, $h_{\mu\mu} \leq 5.0 \cdot 10^{-3}\ \mathrm{GeV}^{-1}\,\mathrm{M_H}$.

Table 7. Summary of the HERA searches for high mass multi-electron events.

experim.	selection	Data	SM expect.
H1	2 e with $M > 100$ GeV	3	0.30 ± 0.05
H1	3 e with $M > 100$ GeV	3	0.23 ± 0.04
ZEUS	2 e with $M > 100$ GeV	2	0.77 ± 0.08
ZEUS	3 e with $M > 100$ GeV	0	0.34 ± 0.09

In H1 a search for high mass multi-electron events has yielded an excess of events at high masses [62], as summarized in Table 7. This observation was initially interpreted as a possible indication for single production of a doubly-charged Higgs. However, in a refined analysis, optimized for doubly-charged Higgs production, one candidate event was selected with an expected SM background of 0.34 events. Also no excess was observed by ZEUS in the multi-electron channel and no excess was found by H1 or ZEUS in the multi-muon channel. Therefore it is considered to be unlikely that the H1 high-mass multi-electron events originate from doubly-charged Higgs production.

Figure 23 summarizes the constraints on doubly-charged Higgs bosons in the plane of Yukawa coupling and doubly-charged Higgs mass. The pair production searches at LEP managed to exclude doubly-charged Higgs bosons up to the kinematic limits of $\sim \sqrt{s}/2$ [63]. The single production limits of doubly-charged Higgses from H1 is shown to depend on the Yukawa coupling and is at masses around $100 - 140$ GeV slightly stronger than the Bhabha scattering limits from SLAC and PETRA [64]. Between $100 - 120$ GeV the effect of the candiate events can be seen. OPAL's analysis on single production of doubly-charged Higgs [65] sets strong limits on the Yukawa coupling for masses between 100 and ~ 160 GeV which are already equivalent to the expected sensitivity from 1 fb^{-1} of HERA-II running. Analysis on Bhabha scattering by OPAL and L3 [66] provides relatively strong limits on the Yukawa coupling up to very high masses.

With analyses based on $91-107$ pb^{-1} CDF and DØ are already now able to exclude doubly-charged Higgs bosons with masses up to ~ 116 GeV [67]. With the expected luminosity of ~ 2 fb^{-1} per experiment in Run-IIA the Tevatron exclusion limit, which is independent of the Yukawa coupling due to the pair production mechanism, is expected to increase up to $150-200$ GeV, covering the entire plane shown in Figure 23.

12 Conclusion

The Standard Model is in various aspects incomplete, giving us strong indications that physics beyond the Standard

Model is to be expected. However, we are presently groping in the dark on where and how we will find it. Fundamental questions on the origin and role of the electroweak, the TeV and the Planck scale remain unanswered. Similarly the origin of the observed particle structure in the lepton and quark sector persists to be a puzzle.

We have a wealth of data in hand, allowing for model-independent searches, searches within numerous models, measurements of rare decays, precision electroweak measurements, and we expect increasing sensitivity from the Tevatron Run-II, HERA-II and eventually from the LHC. So far no significant deviation from the Standard Model expectation has been observed. Nevertheless the strongest indication for new or so far unobserved physics at or from the TeV scale comes from the Higgs sector and electroweak symmetry breaking, where a light Higgs boson appears to be favoured by the presently available dataset. The search goes on at HERA, the Tevatron, and in the future at the LHC or even a linear collider.

Acknowledgements

I would like to thank the organisers of the HEP2003 Europhysics Conference in Aachen, Germany, for their hospitality. I am grateful to many colleagues for their help in preparing this review and for carefully reading this manuscript, in particular to F. Bedeschi, C. Berger, V. Büscher, H. Dreiner, A. Frey, E. Gallo, G. Landsberg, P. Newman, C. Rembser, A. Schöning, T. Wengler, and P. Igo-Kemenes. I do also thank DESY, CERN and Fermilab for the help and support I received as a member of the ZEUS, OPAL, ATLAS and DØ Collaborations.

References

1. EPS'03, P. Wells, Experimental Tests of the Standard Model.
2. EPS'03, S. Arcelli, Search for $H/A \to \mu\mu$ at the LHC; EPS'03, E. Ros, Prospects for Little Higgs Models at the LHC; EPS'03, G. Weiglein, Interplay between the LHC and a Linear Collider in Searches for New Physics; EPS'03, S. Hesselbach, New ideas on SUSY Searches at Future Linear Colliders.
3. K. Hagiwara, S. Komamiya and D. Zeppenfeld, Z.Phys. C29 (1985) 115; U. Bauer, M.Spira and P.M. Zerwas, Phys.Rev. D42 (1990) 815; F. Boudjema, A. Djouadi and J.L. Kneur, Z.Phys. C57 (1993) 425.
4. LEP working group on exotics, LEP Exotica WG 2001-02; ZEUS Collaboration, DESY-01-132, Phys. Lett. B 549 (2002) 32; H1 Collaboration, DESY-02-096, Phys. Lett. B548 (2002) 35; H1 Collaboration, DESY 01-145, Phys. Lett. B 525 (2002) 9.
5. E. Boos et al., hep-ph/011034; O.J.P. Eboli et al., hep-ph/0111001.
6. CDF Collaboration, Phys.Rev.Lett. 72 (1994) 3004; DELPHI Collaboration, CERN-EP/98-169; ZEUS Collaboration; Phys. Lett. B 549 (2002) 32; H1 Collab., Eur. Phys. J. C17 (2000) 567.
7. EPS'03, E. Sanchez, Search for Excited Fermions.
8. W. Buchmüller, R. Rückl and D. Wyler, PHys.Lett.B 191, 442 (1987); erratum in Phys.Lett.B 448, 320 (1999).
9. EPS'03, A. Zarnecki, Search for Leptoquark Production and Lepton Flavour Violation and references therein.
10. H1 Collab., DESY-03-132, Submitted to Eur.Phys.J; ZEUS Collaboration; DESY-03-012, Phys.Lett.B 559 (2003) 153.
11. M. Kuze and Y. Sirois, Search for Particles and Forces Beyond the Standard Model at HERA ep and Tevatron $p\bar{p}$ Colliders, hep-ex/0211048.
12. ALEPH Collaboration, Phys.Lett.B 543 (2002) 173; DELPHI Collaboration, DELPHI 2003-042 CONF 662; L3 Collaboration, Phys.Lett.B 549 (2002) 290; OPAL Collaboration, Phys.Lett.B 521 (2001) 181.
13. CDF Collaboration, Phys.Rev.Lett. 80, 2525 (1998).
14. T. Han et al., hep-ph/9603247, T. Han et al. hep-ph/9506461.
15. Estimate of the HERA-II sensitivity to $\kappa_{tu\gamma} - v_{tuZ}$ in the absence of a signal; D. Dannheim, private communication.
16. EPS'03, J. Ferrando, Single Top Production via FCNC.
17. N. Arkani-Hamed, S. Dimopoulos and G. Dvali, Phys.Lett. B 429, 263 (1009); Phys.Lett.B 436, 257 (1998).
18. L. Randall and R. Sundrum, Phys.Rev.Lett. 83, 3370 (1999); Phys.Rev.Lett. 83, 4690 (1999).
19. G.F. Giudice, R. Rattazzi and J.D. Wells, Nucl.Phys. B 544, 3 (1999).
20. J. Long, J. Price, hep-ph/0303057 and references therein.
21. The OPAL Collaboration, PN 526.
22. The L3 Collaboration, L3 Internal Note 2814.
23. EPS'03, I. Antoniadis, Physics with large extra dimensions; EPS'03, S. Mele, Current experimental bounds on extra dimensions; EPS'03, L. Vacavant, Search for extra dimensions with ATLAS at LHC; EPS'03, F. del Aguila, Extra Dimensions with Brane Localized Kinetic Terms; EPS'03, F. Feruglio, Extra Dimensions in Particle Physics; EPS'03, M. Sanders, Search for Extra Dimensions at Hadron Colliders.
24. EPS'03, P. Azurri, Gaugino Searches and SUSY Models Constraints; EPS'03, M. Wegner, Searches for MSSM/MSUGRA at the Tevatron-II; EPS'03, I. Trigger, Searches for sfermions; EPS'03, S. Hesselbach, New ideas on SUSY Searches at Future Linear Colliders; EPS'03, T. Nunnemann, Search for SUSY in GMSB and AMSB Models; EPS'03, C. Schwanenberger, Search for RPV SUSY.
25. EPS'03, C. Rott, Search for top and bottom squarks.
26. LEP SUSY working group, LEPSUSYWG/01-07.1.
27. D. Hooper, T. Plehn, hep-ph/0212226, Bottino et al., Phys.Rev.D 67, 063519 (2003).
28. H. Dreiner et al., hep-ph/0304289.
29. P.W. Higgs, Phys.Lett 12 (1964) 132; *idem*, Phys.Rev.Lett. 13 (1964) 508; *idem*, Phys.Rev. 145 (1966) 1156; F. Englert and R. Brout, Phys.Rev.Lett. 13 (1964) 321; G.S. Guralnik, C.R. Hagen and T.W.B. Kibble, Phys.Rev.Lett. 13 (1964) 585.
30. The LEP Collaborations ALEPH, DELPHI, L3 and OPAL, the LEP Electroweak Working Group and the SLD Heavy Flavour Group, *A Combination of Preliminary Electroweak Measurements and Constraints on the Standard Model*, CERN-EP/ 2003-02, hep-ex/0312023.
31. The LEP Collaborations ALEPH, DELPHI, L3 and OPAL, the LEP Working Group for Higgs Boson Searches, *Search for the Standard Model Higgs Boson at LEP*, CERN-EP/2003-011, Phys. Letts. B565 (2003) 61-75.

32. B. Klima et al., Tevatron Higgs Sensitivity Working Group, Results of the Tevatron Higgs Sensitivity Study, FERMILAB-PUB-03/320-E.
33. M. Carena et al., Report of the Tevatron Run 2 SUSY/Higgs Working Group, hep-ph/0010338.
34. J. Estrada, Optimal use of Information for Measuring M_t in Lepton+jets $t\bar{t}$ Events, hep-ph/0302031.
35. EPS'03, N. Varelas, Electroweak and Higgs Physics with DØ.
36. ATLAS Collaboration, Detector and Physics Performance Technical Design Report, CERN/LHCC/99-14 (1999); CMS Collaboration, CMS Technical proposal, CERN/LHCC 94-38, CERN (1994).
37. D.L. Rainwater and D. Zeppenfeld, J. High Energy Phys. 12 (1997) 4, hep-ph/9712271; D.L. Rainwater and D. Zeppenfeld, Phys. Rev. D 60 (1999) 113004, hep-ph/9906218.
38. D.L. Rainwater, D. Zeppenfeld and K. Hagiwara, Phys. Rev. D 59 (1999) 14037, hep-ph/9808468; T. Plehn, D.L. Rainwater and D. Zeppenfeld, Phys. Rev. D 61 (2000) 093005.
39. ATLAS Collaboration, Prospects for the Search for a Standard Model Higgs Boson at ATLAS using Vector Boson Fusion; proceedings of Les Houches workshop 2002.
40. K. Mazumdar for the CMS Collaboration, hep-ex/0308070.
41. EPS'03, M. Duersen, Standard Model Higgs Searches at CERN.
42. W. Beenakker et al., Phys. Rev. Lett. 87, (2001) 201805 (hep-ph/0107081); Nucl. Phys. B 653, (2003) 151 (hep-ph/0211352); L. Reina, S. Dawson, Phys. Rev. Lett. 87 (2001) 201804 (hep-ph/0107101); L. Reina, S. Dawson, D. Wackeroth, Phys. Rev. D 65 (2002) 053017 (hep-ph/0109066); S. Dawson et al., Phys. Rev. D 67 (2003) 071503 (hep-ph/0211438); S. Dawson et al., hep-ph/0305087.
43. R. Harlander, W.B. Kilgore, Phys.Rev.Lett. 88 (2002) 201801, Phys.Rev. D68 (2003) 013001; C. Anastasiou, K. Melnikov, Nucl.Phys. B646 (2002) 220; V. Ravindran, J. Smith, W. van Neerven, Nucl.Phys. B634 (2002) 247, Nucl.Phys. B665 (2003) 325.
44. T. Binoth et al., Phys. Rev. D 63 (2001) 114016 (hep-ph/0012191).
45. C. Campbell et al., Phys. Rev. D 67 (2003) 095002 (hep-ph/0204093).
46. M.L. Ciccolini, S. Dittmaier, M. Krämer, hep-ph/0306234.
47. The LEP-Higgs Working Group, Searches for the Neutral Higgs Boson of the MSSM: Preliminary Combined Results Using LEP Data Collected at Energies up to 209 GeV, LHWG-Note 2001-04.
48. M. Carena et al., Suggestions for Benchmark Scenarios for MSSM Higgs Boson Searches at Hadron Colliders, hep-ph/0202167.
49. OPAL Collaboration, PN524.
50. EPS'03, P. Bechtle, Search for SUSY Neutral Higgs and interpretations.
51. A. Pilaftsis and C.E. Wagner, Nucl. Phys. B 553 (1999) 3.
52. M. Carena et al., Nucl. Phys. B 599 (2001) 158.
53. LEP-Higgs working group, Search for Charged Higgs bosons: Preliminary Combined Results Using LEP Data Collected at Energies up to 209 GeV, LHWG Note/2001-05.
54. L3 Collaboration, L3 note 2817.
55. OPAL Collaboration, CERN-EP/2002-085; Phys. Lett. B 551 (2003) 35.
56. DELPHI Collaboration, DELPHI 2003-038 CONF 658.
57. EPS'03, J. Cuevas, Search for (Singly and Doubly) charged Higgses.
58. LEP-Higgs working group, Searches for Higgs Bosons Decaying into Photons: Combined Results from the LEP Experiments LHWG Note/2002-02.
59. CDF Collaboration, Phys. Rev. D 59 (1999) 092002; DØ Collaboration, Phys. Rev. Lett. 82 (1999) 2244.
60. DELPHI Collaboration, DELPHI 2003-043 CONF 663.
61. EPS'03, D. Baden, Fermiophobic Higgs Searches.
62. H1 Collab., A. Aktas et al., Accepted by Eur.Phys.J.
63. DELPHI Collaboration, Phys. Lett. B 552 (2003) 127; OPAL Collaboration, Phys. Lett. B 526 (2002) 221; L3 Collaboration, L3 note 2818.
64. M.L. Swartz, Phys. Rev. D 40 (1989) 1521.
65. The OPAL Collaboration, CERN-EP-2003-041, Accepted by Phys.Lett.B.
66. OPAL Collaboration, CERN-EP-2003-041, Accepted by Phys Lett. B.; L3 Collaboration, CERN-EP/2003-060.
67. CDF Collaboration, CDF note 6342, DØ Collaboration, DØ-Note 4217.